Desalination and Water Treatment
www.deswater.com
doi: 10.1080/19443994.2016.1157044

57 (2016) 25686–25695
November

Effects of nitrite anions and ammonium cations on the photolysis of bisphenol S in nitrate solution

Guiping Cao*, Jintao Zhang, Baoliang Liu

Department of Chemical Engineering, Changzhou Institute of Technology, Changzhou 213022, China, emails: caogpczu@163.com (G. Cao), zhangjt@czu.cn (J. Zhang), liubl@czu.cn (B. Liu)

Received 19 October 2015; Accepted 3 February 2016

ABSTRACT

The effects of nitrate ions on the photolysis of bisphenol S (BPS) under UV irradiation were studied using reaction kinetics. Based on this research, we investigated how nitrite anions and ammonium cations codissolved with nitrate affected the UV photolysis of BPS. The BPS photolysis fitted well to a first-order kinetic equation, and the half-life of BPS photolysis varied with changes in pH value, shortening from 95.0 min at pH 2 to 42.3 min at pH 10. Nitrate added to the BPS solution inhibited the BPS photolysis, but the extent of the inhibitory effect was associated with the pH value of the aqueous solution. The inhibiting ratio remained within 19.2–27.6% in acidic and neutral solutions, while it stayed at about 3.6% in alkaline solutions. Nitrite anions exhibited a strong inhibitory effect on BPS photolysis, but the inhibitory effect of NO_2^- coexistent in a BPS-NO_3^- solution was weaker than that of separate NO_2^-, indicating that the inhibitory effect of mixed form of NO_2^- and NO_3^- were not simply additive; some offset might exist between them. Ammonium cations had no effect on BPS photolysis, but NH_4^+ codissolved in NO_3^- solution weakened the inhibition of NO_3^-, thus indirectly promoting BPS photolysis in NO_3^- solution. When 32 mg/L NH_4^+ was added to a BPS-NO_3^- solution, the coexistent NH_4^+ exhibited a promoting effect on BPS photolysis, and the promoting ratio reached 5.3% at 64 mg/L NH_4^+. The mechanisms of BPS photolysis under the presence of nitrate ions were also discussed.

Keywords: Bisphenol S; Photolysis; Nitrate; Nitrite anions; Ammonium cations

1. Introduction

As evidence regarding the toxic effects of bisphenol A (BPA) grows, its application in commercial products is gradually being replaced with other related compounds, such as bisphenol S (BPS, 4,4′-sulfonyldiphenol) [1]. In 2011, the European Commission restricted the use of BPA in plastic infant feeding bottles. Because of this restriction, BPS is now often used as the component of choice for plastic substitutes in the production of baby bottles [2]. As a new type of chemical raw material, many of BPS's properties and uses are superior to those of BPA, especially in aggregation and in its ability to improve the mechanical properties and thermal stability of polymer products [3,4]. The development and application of BPS is gradually catching up to and even surpassing that of BPA. As a result, this compound's widespread application has increased the risk of human exposure to BPS, which is found not only in many paper products [5], such as thermal receipt papers, paper currencies,

---

*Corresponding author.

magazines, newspapers, food contact papers, and toilet paper, but also detected in food cans [6] and human urine samples collected in the United States and in seven Asian countries [7].

As demonstrated by a green fluorescent protein expression system, BPS shows estrogenic activity that is comparable with BPA [8] and is potentially harmful to human health. An understanding of the fate of BPS in the aquatic environment is therefore vital for assessing its environmental impact and potential health threats. Among various transformation processes, photolysis is an important factor influencing the fate of organic pollutants in aquatic environments [9]. Several studies have reported on the behavioral characteristics of BPS photolysis in aqueous solutions and the effect of surfactants [10,11]. However, the influence of nitrate ions on the BPS photolysis is poorly documented.

Nitrate is a ubiquitous pollutant in both natural water and drinking water [12–14]. Some nitrate ions may be transformed into nitrite anions by denitrification [15] or photolysis [16]. Moreover, some ammonium cations can be formed in a solution containing nitrite anions under sunlight illumination [17]. Several authors have reported the influences of nitrate ions [18,19] and nitrite anions [20,21] on the photodecomposition of different organic pollutants. However, reports on the effect of ammonium cations on the photolysis of organic pollutants are limited, and there are even fewer reports on the effects of nitrite anions or ammonium cations coexisting in a nitrate solution.

This paper aims at using photolysis kinetics to determine the effects of nitrate solutions having different pH values on BPS photolysis under UV light irradiation, and the effects of nitrite anions and ammonium cations co-dissolved with nitrate solutions are further investigated respectively. Our results can provide a theoretical basis for the treatment and environmental remediation of eutrophic water containing BPS.

2. Materials and methods

2.1. Chemicals

Analytical-grade BPS was obtained from Beijing Chemical Reagent Co., Ltd (China). High-performance liquid chromatography (HPLC)-grade acetone and ethyl acetate were obtained from Tedia Ltd (Fairfield, USA). Terephthalic acid was purchased from Fluka Ltd (Sigma-Aldrich, USA). Analytical-grade ethyl acetate and anhydrous sodium sulfate were obtained from Sinopharm Chemical Reagent Co., Ltd (Shanghai, China) and used to treat samples in the identification of transformation products. Sodium nitrate ($NaNO_3$), sodium nitrite ($NaNO_2$), and ammonium sulfate ($(NH_4)_2SO_4$) were purchased from Shanghai Laboratory Reagent Co., Ltd (China) and used to provide the nitrate ions, nitrite anions, and ammonium cations used in this study, respectively.

A 50 mg/L BPS stock solution was prepared by dissolving 0.0250 g of BPS in an ultrasonic cleaner (KH-500B, Kunshan), diluting with water into a 500-mL volumetric flask. A 1,000 mg/L NO_3^- stock solution was prepared by dissolving 0.6855 g of $NaNO_3$ in 500 mL of water. A 500 mg/L NO_2^- stock solution was prepared by dissolving 0.1875 g of $NaNO_2$ in 250 mL of water. A 500 mg/L NH_4^+ stock solution was prepared by dissolving 0.4584 g of $(NH_4)_2SO_4$ in 250 mL of water. All stock solutions were refrigerated at 4℃ after preparation and used within one month. Working solutions with different concentrations were freshly prepared by diluting the corresponding stock solution with water before use. Aqueous solutions having pH values of 2 and 10 were made using a pH meter (Thermo Orion, USA) and adjusting the solutions as needed with 0.1 mol/L H_2SO_4 or 0.1 mol/L NaOH. All experimental solutions were prepared with double-distilled water.

2.2. Photolysis experiments

Photolysis experiments were carried out in a self-made reactor. A 20 W UV lamp with an irradiation wavelength of 254 nm (Yuelu Irradiation Lamp Co., Ltd, Changsha, China) was hung over a quartz tube (outer diameter 1.8 cm; length 13.5 cm) at a fixed distance of 6.0 cm. The temperature of the reactor was maintained at 25 ± 1℃.

A set of 15 mg/L BPS solutions with different concentrations of added NO_3^- ions (NO_2^- anions, or NH_4^+ cations) was prepared, placed in the quartz tubes, and irradiated under the UV lamp. Samples were collected at 20-min intervals, and the residual BPS concentrations were measured by HPLC. To minimize errors, all experiments were performed in triplicate and the average results were calculated.

2.3. Measurement of absorption spectra

In this study, the UV absorption spectra of BPS in different solutions were obtained using a UV-1102 spectrophotometer (Shanghai Techcomp Instrument Ltd, China) scanning between 210 and 350 nm.

2.4. Analytical methods

BPS concentration during photolysis was measured by an HPLC system (Agilent 100, USA) using a device fitted with a Discovery C18 reversed-phase column (150 × 4.5 mm, 5 μm) at 30℃. The mobile phase composition was ethyl acetate-acetone (60:40, V/V) at a flow rate of 1.0 mL/min. Samples were analyzed with a UV detector at a wavelength of 258 nm. The retention time of BPS under these chromatographic conditions was 18.7 min. Measurements were performed in triplicate for each experiment with less than 5% error.

For analyzing hydroxyl radicals produced in the process of BPS photolysis, 5 mg/L terephthalic acid was added to each solution containing BPS before the UV irradiation process. Every 15 min, 5 mL of the photolyzed solution was collected to determine its emission spectrum, ranging between 340 and 560 nm, with an F-4600 fluorescence spectrophotometer (Shanghai Techcomp Instrument Ltd, China) at an excitation wavelength of 315 nm. The maximum emission wavelength of the fluorescent material produced was 425 nm.

To identify the intermediate products produced in the process of BPS photolysis under the presence of nitrate ions, the photolyzed solutions (600 mL) were extracted with ethyl acetate for three times to allow better extraction. The organic extracts were decreased to 3 mL in a rotary evaporator (Yarong, Shanghai, China) under the following conditions: room temperature, 0.09 MPa vacuum pressure, and 75 r/min rotating speed. The concentrated liquid was dried by anhydrous sodium sulfate and analyzed by GC/MS using an Agilent 7890A/5975C GC/MS equipped with a 30 mm × 0.25 mm × 0.25 μm DB-5MS column. Helium was used as the carrier gas with a flow rate of 1.0 mL/min. The GC oven temperature was held at 50℃ for 3 min and then the temperature programmed at 30℃/min to 290℃ holding the final temperature for 9 min. A volume of 1 μL of sample was injected in the splitless mode at an injector temperature of 270℃. The transfer line and ion source were set at 280 and 230℃, respectively. The MS was operated in electron ionization mode with a potential of 70 eV and the spectra were obtained in full scan mode from m/z 20–400.

2.5. Data analysis

Reaction kinetics was examined by studying the concentration vs. time plots. The photolysis of BPS in different solution followed a first-order kinetic equation well, and the concentration of the solution was available on the kinetic equation [22], as shown in Eq. (1):

$$C = C_0\, e^{-kt} \tag{1}$$

where C_0 is the initial BPS concentration, C is the residual BPS concentration at time t, k is the photolysis rate constant, and t is the irradiation time. The rate constant k was obtained by using the corresponding regression equation, as shown in Eq. (2):

$$\ln(C/C_0) = -kt \tag{2}$$

The time required to complete 50% of the BPS photolysis is called the photolysis half-life ($t_{1/2}$) and was determined by Eq. (3):

$$t_{1/2} = \ln 2/k \tag{3}$$

The effect of the coexisting ions on BPS photolysis was analyzed as in Eq. (4):

$$\text{Promoting (Inhibiting) ratio (\%)} = (k_\mathrm{i} - k_0)/k_0 \times 100 \tag{4}$$

where k_0 is the photolysis rate constant of the pure BPS solution and k_i is the rate constant of BPS in the mixture. A positive value for this ratio indicates a promoting effect of the ion on BPS photolysis, whereas a negative value indicates an inhibitory effect.

3. Results and discussion

3.1. BPS photolysis in nitrate solution

UV photolysis for BPS was first conducted in pure water. Fig. 1 shows that BPS concentrations were not significantly changed in reactions carried out in the dark, while BPS photodegraded rapidly under UV light irradiation. The BPS photolysis fitted to the first-order kinetic equation well, and the regression

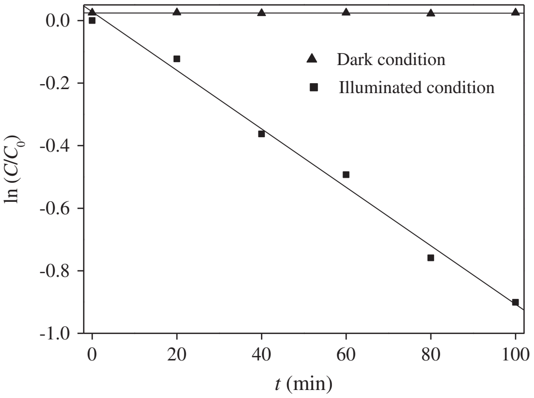

Fig. 1. Comparison of BPS photolysis in pure water under dark and illuminated condition. Experimental conditions: 15 mg/L BPS, no NO_3^- ions, no pH adjustment.

equation is $\ln(C/C_0) = 0.0278–0.0094t$, in which the correlation coefficient was 0.991. The photolytic half-life $t_{1/2}$ was 73.7 min.

The effects of nitrate ions with different concentrations on BPS photolysis were presented in Table 1. NO_3^- exhibited an inhibitory effect on BPS photolysis. The half-life of BPS photolysis rapidly increased with increased NO_3^- concentrations and reached 93.6 min at 32 mg/L. Thereafter, the half-life slowly increased with further increased in NO_3^- concentration. At 64 mg/L NO_3^-, the half-life of BPS only increased to 101.9 min. At concentrations ranging from 4 to 32 mg/L, NO_3^-'s inhibiting ratio for BPS photolysis rapidly increased, almost by a factor of 20 times, from 1.1 to 21.3%. Finally, at 32–64 mg/L NO_3^-, its inhibiting ratio remained within the 21.3–27.6% range, and NO_3^-'s inhibitory effect showed a stable trend. Therefore, we selected a concentration of 64 mg/L NO_3^- to carry out the following studies.

Photolysis can be direct, whereby the organic pollutant directly absorbs photons and then undergoes degradation, or it can be indirect [23,24]. A series of photochemical reactions may lead to the formation of reactive oxygenated radicals, mainly the hydroxyl radical (·OH), which can lead to indirect photolysis [25]. Capturing an ·OH radical using a chemical capture agent is currently the main method used to detect the presence of ·OH radicals [26]. Using terephthalic acid as the ·OH radical capture agent, a fluorescence spectrum technique was employed to examine whether ·OH can be produced during the BPS photolysis process. Fig. 2 shows that terephthalic acid and BPS were not fluorescent. The fluorescence intensity value of the BPS solution at 425 nm was only 75 (as a blank value) at 0 min illumination. With the extension of photolysis time, the fluorescence intensity of the BPS photolysis solution increased gradually. Terephthalic acid, when attacked by an ·OH radical, will react and produce 2-hydroxy-terephthalate, which can generate a fluorescence signal [27].

This shows that ·OH radicals were produced in the BPS photolysis process. Therefore, we can conclude that BPS photolysis involves not only direct but also indirect photolysis. The fluorescence intensity value ΔF, after deducting the blank value, was linear with the photolysis time t. The linear relationship can be described as follows (Eq. (5)):

$$\Delta F = 174.6 + 68.46t\,(\text{min}) \tag{5}$$

The correlation coefficient in Eq. (5) is 0.992. The apparent reaction rate constant is $K = \Delta F/t = 1.14\ \text{s}^{-1}$. However, when 64 mg/L NO_3^- was added to this system, the fluorescence intensity values detected at the corresponding photolysis times were lower than those in the same system without the 64 mg/L NO_3^-. The linear relationship between ΔF and t was measured as follows (Eq. (6)):

$$\Delta F = 161.0 + 52.92t\,(\text{min}) \tag{6}$$

The correlation coefficient in Eq. (6) is 0.990. The apparent reaction rate constant is $K = 0.88\ \text{s}^{-1}$, only 0.77 times the reaction rate constant without the NO_3^-. This indicates that the added nitrate inhibited the generation of ·OH radicals during the BPS photolysis process by acting as an ·OH scavenger, thus reducing the photolysis rate in the BPS solution. This inhibition was consistent with that of the nitrate-hindered di(2-ethylhexyl) phthalate degradation reported by Park et al. [28].

The UV absorption spectra of BPS solutions having 0 and 64 mg/L NO_3^- were shown in Fig. 3(a) and (c). The BPS spectrum revealed two maxima at 234 and 258 nm. However, after NO_3^- was added to the

Table 1
Photolytic constants of BPS in NO_3^- solution under different pH values. Experimental conditions: 15 mg/L BPS, no pH adjustment in the pH 6 solution

pH	NO_3 (mg/L)	Regression equation	k (min^{-1})	$t_{1/2}$ (min)	Correlation coefficient	Inhibiting ratio (%)
6	0	$\ln(C/C_0) = 0.0278–0.0094t$	0.0094	73.7	0.991	–
	4	$\ln(C/C_0) = 0.0203–0.0093t$	0.0093	74.5	0.996	−1.1
	8	$\ln(C/C_0) = 0.0299–0.0085t$	0.0085	81.5	0.995	−9.6
	32	$\ln(C/C_0) = 0.0082–0.0074t$	0.0074	93.6	0.988	−21.3
	64	$\ln(C/C_0) = 0.0001–0.0068t$	0.0068	101.9	0.996	−27.6
2	0	$\ln(C/C_0) = 0.0568–0.0073t$	0.0073	95.0	0.980	–
	64	$\ln(C/C_0) = 0.0256–0.0059t$	0.0059	117.5	0.989	−19.2
10	0	$\ln(C/C_0) = 0.0628–0.0164t$	0.0164	42.3	0.994	–
	64	$\ln(C/C_0) = 0.0551–0.0158t$	0.0158	43.8	0.993	−3.6

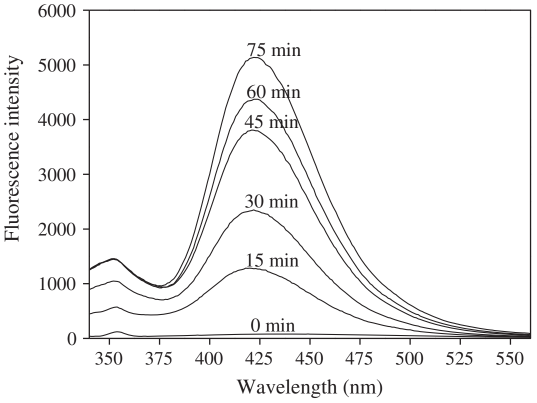

Fig. 2. Fluorescence spectral changes observed during illumination of BPS in 5 mg/L terephthalic acid solution. Experimental conditions: 15 mg/L BPS, no NO_3^- ions, no pH adjustment, excitation at 315 nm.

solution, the absorption peak at 234 nm disappeared due to NO_3^- absorption. Nitrate absorption of UV light was stronger than that of BPS between the wavelengths of 210–250 nm. Changes in the BPS solutions' absorption spectra may be another main reason for the inhibitory effect of NO_3^- on BPS photolysis. The addition of NO_3^- enhanced the UV absorption of the solution at wavelengths <250 nm and competed with BPS for the absorption of photons, and further affected the direct photolysis of BPS, thereby decreasing the BPS photolysis rate.

The pH value of the pure BPS solution was six. The solution pH value was adjusted to 2 and 10 with sulfuric acid and sodium hydroxide, respectively. We then examined the effect of different pH values on BPS photolysis in a NO_3^- solution and the results are also presented in Table 1. We found that the photolysis rates of the pure BPS solutions were not the same as those with different pH values. In fact, they increased with an increase in pH value. The half-life of BPS photolysis rapidly decreased from 95.0 to 42.3 min as the pH value increased from 2 to 10. When 64 mg/L NO_3^- was added, the half-life of BPS photolysis changed in a different direction, being prolonged from 95.0 to 117.5 min in pH 2 solutions and from 73.7 to 101.9 min in pH 6 solutions. However, in the solution having a pH value of 10, the half-life of BPS photolysis was only prolonged from 42.3 to 43.8 min. These results indicate that the inhibitory effect of nitrate on BPS photolysis varied with the pH value of the solution. The inhibitory effect was stronger in acidic and neutral solutions, with the inhibiting ratio remained between 19.2 and 27.6%. The inhibitory effect was relatively weaker in an alkaline solution, where the inhibiting ratio remained at about 3.6%.

Fig. 4 shows there was almost no difference in the UV absorption spectra of BPS solutions at acidic and neutral pH values. However, the OH^- ion concentration in a pH 6 solution was 10,000 times than that in the pH 2 solution. The OH^- ion helps to induce the generation of the ·OH radical, the main ingredient of photocatalytic photolysis [29]. Therefore, the half-life of BPS photolysis decreased from 95.0 min in a pH 2 solution to 73.7 min in a pH 6 solution, a reduction of 22.4%. Nitrate ions inhibited BPS photolysis because of its absorption of UV light in the wavelength range of 210–250 nm, and the inhibiting ratio remained

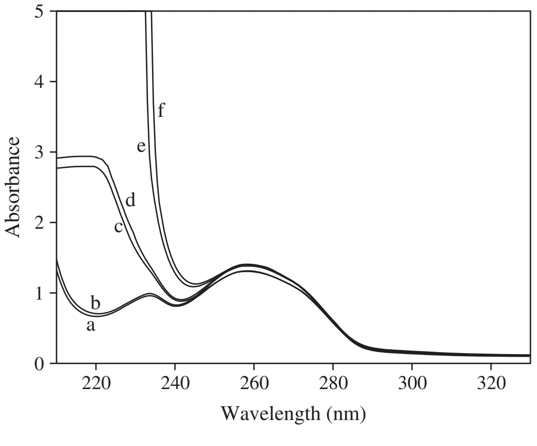

Fig. 3. UV absorption spectra of BPS solutions with different coexistent ions. (a) BPS, (b) BPS + NH_4^+, (c) BPS + NO_3^-, (d) BPS + NO_3^- + NH_4^+, (e) BPS + NO_2^-, and (f) BPS + NO_3^- + NO_2^-. Experimental conditions: 15 mg/L BPS, 64 mg/L NH_4^+, 64 mg/L NO_3^-, 64 mg/L NO_2^-, no pH adjustment.

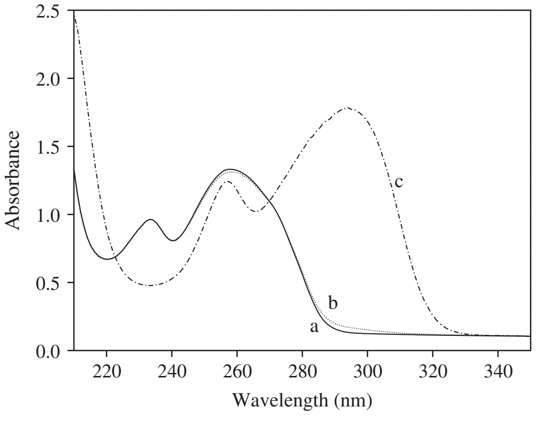

Fig. 4. UV absorption spectra of BPS solutions with different pH values. (a) pH 2, (b) pH 6, and (c) pH 10. Experimental conditions: 15 mg/L BPS, no NO_3^- ions, no pH adjustment in the pH 6 solution.

within 19.2–27.6%. In an alkaline solution, the two absorbance peaks at 234 and 258 nm shifted to 258 and 295 nm, respectively, and the absorption intensity also increased correspondingly. Therefore, the half-life of BPS photolysis decreased from 73.7 min in a pH 6 solution to 42.3 min in a pH 10 solution, a reduction of 42.6%. However, nitrate hardly absorbs UV light at all at wavelengths >250 nm, weakening its inhibition of the direct BPS photolysis in alkaline solutions. Meanwhile, a large number of OH^- ions helped to generate more $^{\cdot}OH$ radicals, which then weakened the nitrate's inhibitory effect on the indirect photolysis of BPS. Thus, the inhibitory effect of nitrate ions was very weak in alkaline solutions. The half-life of BPS photolysis in a 64 mg/L NO_3^- solution with a pH value of 10 increased from 42.3 to 43.8 min, an increase of only 3.5%.

3.2. *Effect of coexistent nitrite anions*

The effects of nitrite anions with different concentrations on BPS photolysis in NO_3^- solution are presented in Table 2. NO_2^- exhibited an inhibitory effect on BPS photolysis regardless of the presence or absence of NO_3^- in the solution. Some studies indicate that NO_2^- anions quench $^{\cdot}OH$ radicals in an aqueous solution through the photochemical reaction equations shown in Eqs. (7) and (8) [30,31], and therefore, a reduction of $^{\cdot}OH$ radicals resulted in the decrease in the indirect BPS photolysis rate.

$$NO_2^- + {}^{\cdot}OH \rightarrow NO_2^{\cdot} + OH^- \qquad (7)$$

$$2NO_2^{\cdot} \rightarrow N_2O_4 \qquad (8)$$

However, the extent of the inhibitory effect of NO_2^- on BPS photolysis was associated with its own state and concentration. When NO_2^- and NO_3^- existed separately in BPS solutions, the inhibiting ratio produced by 8 mg/L NO_2^- was 27.6%, as large a percentage as that produced by a 64 mg/L NO_3^- solution. This indicates that the inhibitory effect of NO_2^- was stronger than that of NO_3^- when in a separate state. When NO_2^- was added to the BPS-NO_3^- solution, the inhibitory effect of NO_2^- was closely linked to its concentration. When 8 mg/L NO_2^- was added to the BPS-NO_3^- solution, an inhibiting ratio of 33.0% was produced, only increasing 5.4% from the 27.6% measured when separate; when 32 and 64 mg/L NO_2^- were added to the BPS-NO_3^- solution, the inhibiting ratio produced was 48.9 and 62.8%, an increase of 21.3 and 35.2% from 27.6%, respectively. This indicates that the inhibitory effect of coexistent NO_2^- was enhanced with an increased NO_2^- concentration in the BPS-NO_3^- solution, but the inhibitory effect of coexistent NO_2^- was weaker than that of separate NO_2^-. The inhibitory effects of mixed form of NO_2^- and NO_3^- on BPS photolysis were not simply additive; an offset effect might exist between them.

When 64 mg/L NO_2^- and NO_3^- were added to the BPS solution, respectively, large changes appeared in the UV absorption curves, as shown in Fig. 3 (*c*, *e* and *f*). The absorption property of curve *e* was much stronger than that of curve *c* in the wavelength range of 210–250 nm. Therefore, the inhibitory effect of NO_2^- on direct BPS photolysis was stronger than that of NO_3^- existing in the BPS solution independently. However, if the same concentration of NO_2^- was added to the BPS-NO_3^- solution, the absorption curve of the solution did not change significantly, as indicated by curve

Table 2
Effects of coexistent ions on photolytic constants of BPS in NO_3^- solution. Experimental conditions: 15 mg/L BPS, no pH adjustment

NO_3^- (mg/L)	NO_2^- (mg/L)	NH_4^+ (mg/L)	Regression equation	k (min^{-1})	$t_{1/2}$ (min)	Correlation coefficient	Inhibiting (Promoting) ratio (%)
0	0	0	$\ln(C/C_0) = 0.0278–0.0094t$	0.0094	73.7	0.991	–
0	8	0	$\ln(C/C_0) = 0.0336–0.0068t$	0.0068	101.9	0.990	−27.6
64	0	0	$\ln(C/C_0) = 0.0001–0.0068t$	0.0068	101.9	0.996	−27.6
64	8	0	$\ln(C/C_0) = 0.0090–0.0063t$	0.0063	110.0	0.998	−33.0
64	32	0	$\ln(C/C_0) = 0.0495–0.0048t$	0.0048	144.4	0.962	−48.9
64	64	0	$\ln(C/C_0) = 0.0116–0.0035t$	0.0035	198.0	0.990	−62.8
0	0	4	$\ln(C/C_0) = 0.0413–0.0094t$	0.0094	73.7	0.988	0
64	0	4	$\ln(C/C_0) = 0.0284–0.0076t$	0.0076	91.2	0.994	−19.1
64	0	8	$\ln(C/C_0) = 0.0060–0.0083t$	0.0083	83.5	0.996	−11.7
64	0	32	$\ln(C/C_0) = 0.0350–0.0095t$	0.0095	72.9	0.984	+1.1
64	0	64	$\ln(C/C_0) = 0.0531–0.0099t$	0.0099	70.0	0.993	+5.3

f. When the absorption of NO_2^- and NO_3^- was included, the absorption intensity of curve *f* at wavelengths <250 nm was only slightly stronger than that of curve *e*. Thus, the inhibitory effect of coexistent NO_2^- on BPS photolysis in NO_3^- solution was weaker than that in the same BPS solution without NO_3^-.

3.3. Effect of coexistent ammonium cations

The effects of ammonium cations on BPS photolysis in a NO_3^- solution were also presented in Table 2. The half-life of BPS photolysis remained the same whether NH_4^+ was added to the BPS solution. This suggests that NH_4^+ in itself did not have any impact on BPS photolysis. However, when NH_4^+ was added to a BPS-NO_3^- solution, the half-life of BPS photolysis changed a great deal. When 4 mg/L NH_4^+ was added to the BPS-NO_3^- solution, the half-life of BPS photolysis reduced from 101.9 to 91.2 min, and the inhibiting ratio produced by the NH_4^+ cations codissolved with NO_3^- was 19.1%, a decrease in 8.5% from 27.6% measured in the 64 mg/L NO_3^- solution. The inhibitory effect of NO_3^- in the solution system decreased significantly. When 32 mg/L NH_4^+ was added to a BPS-NO_3^- solution, the coexistent NH_4^+ exhibited a promoting effect on BPS photolysis, and at 64 mg/L NH_4^+, its promoting ratio was 5.3%. This indicates that there may be an interaction between NH_4^+ and NO_3^-, which weakened the inhibition of NO_3^- as shown earlier. Therefore, NH_4^+ coexisting in BPS-NO_3^- solution can promote BPS photolysis, and the promoting effect increased with an increasing NH_4^+ concentration.

Fig. 3 shows that absorption curve *b* with added NH_4^+ cations did not produce significant differences from absorption curve *a*. This indicates that NH_4^+ cations hardly absorb photons within the wavelength range of BPS absorption, and thus had no influence on BPS photolysis. Similarly, no significant differences were found when comparing curves *c* and *d* either. However, NH_4^+ cations promoted the photolysis of BPS in the NO_3^- solution. As mentioned in Section 3.1, adding NO_3^- to the solution can inhibit the generation of ·OH radicals in the BPS photolysis process. However, when NH_4^+ was added to the BPS-NO_3^- solution, its acidity increased, making conditions conducive to the occurrence of a photochemical reaction (9) [31]. The ·OH radicals produced in reaction (9) promoted the indirect photolysis of BPS.

$$NO_3^- + H^+ \xrightarrow{hv} {}^{\cdot}NO_2 + {}^{\cdot}OH \tag{9}$$

The ·OH radicals produced in BPS-NO_3^- solutions with different concentrations of NH_4^+ cations were then determined at different illumination times, and results are shown in Fig. 5. The fluorescence intensity values of the solutions increased with increasing NH_4^+ concentrations in BPS-NO_3^- solutions. This demonstrates that the ·OH radicals produced in BPS-NO_3^- solution systems increased as the NH_4^+ concentrations increased, which then increased the rate of BPS photolysis in NO_3^- solution.

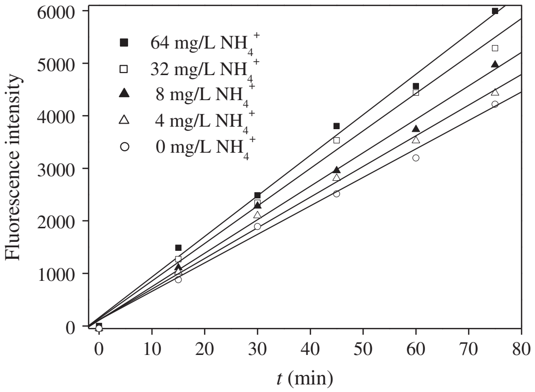

Fig. 5. Fluorescence intensity changes in BPS-NO_3^- solution systems with different concentration of NH_4^+ cations. Experimental conditions: 15 mg/L BPS, 64 mg/L NO_3^-, 5 mg/L terephthalic acid, no pH adjustment.

When 64 mg/L NH_4^+ was added to the BPS-NO_3^- solution, the linear relationship between ΔF and t was measured as follows (Eq. (10)):

$$\Delta F = 160.6 + 77.18t\,(\text{min}) \tag{10}$$

The correlation coefficient in Eq. (10) is 0.994. The apparent reaction rate constant K is 1.29 s^{-1}, more 1.46 times the reaction rate constant without the NH_4^+. Therefore, although NH_4^+ cations alone did not affect BPS photolysis, when NH_4^+ and NO_3^- coexisted in BPS solutions, the inhibitory effect of NO_3^- ions was impaired by NH_4^+ cations and thus NH_4^+ cations indirectly promoted BPS photolysis in NO_3^- solution.

3.4. Proposed mechanisms of BPS photolysis in nitrate solution

The 30 mg/L BPS solution containing 32 mg/L NO_3^- was under UV irradiation for 70 min, and GC/MS analysis of the irradiated solution was performed. The intermediate products were identified by GC/MS with headspace injection systems, and some products with an high-boiling temperature might not be identified. Eight compounds could be identified as possible degradation products during the BPS

Table 3
GC/MS analysis results for intermediates of BPS photolysis in nitrate solution

Number	Retention time (min)	Product	m/z
1	6.156	1,4-Benzoquinone	110, 108, 82, 80, 54, 37
2	6.614	Benzaldehyde	106, 105, 77, 51, 50, 37
3	6.781	Phenol	94, 78, 66, 65, 55, 39
4	7.447	2-Phenylacetaldehyde	120, 92, 91, 65, 43
5	8.068	Catechol	110, 92, 81, 64, 63, 53
6	8.226	Naphthalene	128, 127, 102, 87, 64, 51
7	9.257	Benzoic acid	122, 117, 105, 77, 43
8	10.444	L(+)-Mandelic acid	152, 121, 107, 79, 77, 57, 43

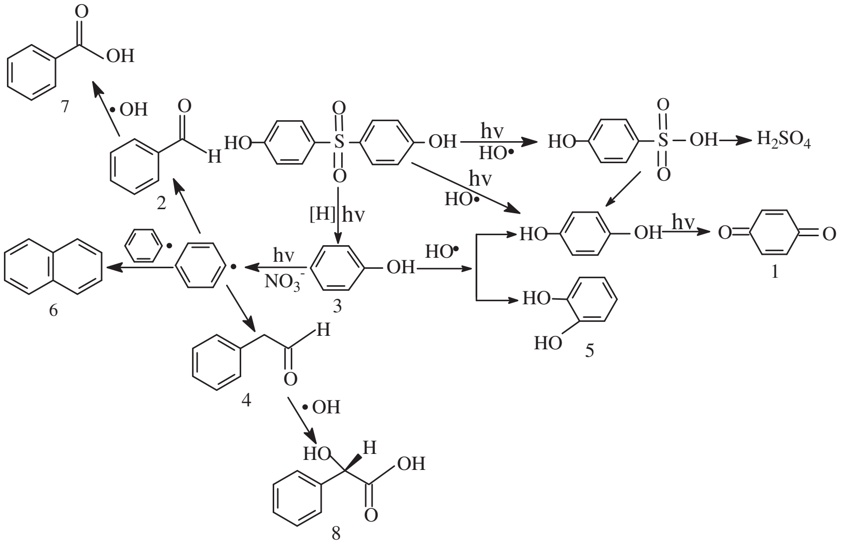

Fig. 6. Proposed photodegradation pathways of BPS in nitrate solution.

photodegradation process in nitrate solution. Their major GC/MS characteristics are summarized in Table 3.

On the basis of above experimental data, a possible photodegradation pathway of BPS in NO_3^- solution can be inferred as shown in Fig. 6. Hydroquinone, phenol-4-sulfonic acid and sulfuric acid has been depicted in the previous study [11], which were not detected because of their low concentrations or high-boiling temperatures. Products 1 and 5, 1,4-benzoquinone and catechol, can be also observed in the phenol (product 3) degradation process [32,33]. In this experiment, photoproducts 2, 4, 6, 7, and 8 were observed, which might be attributed to the addition of nitrate ions in the BPS solution. The nitrate ions can not only capture hydroxyl radicals in the solution, inhibiting the indirect photolysis of BPS, but also hydroxyl radicals in the phenol, leading to the formation of phenyl radicals.

4. Conclusions

Photolysis experiments described in this work demonstrated that the photolysis of BPS under UV irradiation followed a first-order kinetics equation. Nitrate inhibited BPS photolysis in acidic or neutral solutions; however, this inhibition did not occur in alkaline solutions. Nitrite anions coexisting in the NO_3^- solution also inhibited BPS photolysis, but its inhibitory effect was weaker than that in a separate state because of the interaction between the two ions. Although ammonium cations showed no effect on BPS photolysis, when coexisting in the NO_3^- solution, they weakened the inhibitory effect of NO_3^- and thus indirectly promoted BPS photolysis.

Acknowledgements

This research was supported by Jiangsu Province Key Laboratory of Environmental Engineering

(KF2014010). The authors would like to extend their gratitude to M.S. Wen-Juan Yu at the Instrumental Analysis Center of SJTU (Shanghai, China) for photoproduct analysis.

References

[1] C. Héliès-Toussaint, L. Peyre, C. Costanzo, M.C. Chagnon, R. Rahmani, Is bisphenol S a safe substitute for bisphenol A in terms of metabolic function? An *in vitro* study, Toxicol. Appl. Pharmacol. 280 (2014) 224–235.

[2] E. Grignard, S. Lapenna, S. Bremer, Weak estrogenic transcriptional activities of bisphenol A and bisphenol S, Toxicol. In Vitro 26 (2012) 727–731.

[3] N. Lotti, M. Colonna, M. Fiorini, L. Finelli, C. Berti, Poly(butylene terephthalate) modified with ethoxylated bisphenol S with increased glass transition temperature and improved thermal stability, Polymer 52 (2011) 904–911.

[4] X.F. Li, H. Na, H. Lu, Novel sulfonated poly(ether ether ketone ketone) derived from bisphenol S, J. Appl. Polym. Sci. 94 (2004) 1569–1574.

[5] C.Y. Liao, F. Liu, K. Kannan, Bisphenol S, a new bisphenol analogue, in paper products and currency bills and its association with bisphenol a residues, Environ. Sci. Technol. 46 (2012) 6515–6522.

[6] P. Viñas, N. Campillo, N. Martínez-Castillo, M. Hernández-Córdoba, Comparison of two derivatization-based methods for solid-phase microextraction-gas chromatography–mass spectrometric determination of bisphenol A, bisphenol S and biphenol migrated from food cans, Anal. Bioanal. Chem. 397 (2010) 115–125.

[7] C.Y. Liao, F. Liu, H. Alomirah, V.D. Loi, M.A. Mohd, H.B. Moon, H. Nakata, K. Kannan, Bisphenol S in urine from the United States and Seven Asian countries: Occurrence and human exposures, Environ. Sci. Technol. 46 (2012) 6860–6866.

[8] R. Kuruto-Niwa, R. Nozawa, T. Miyakoshi, T. Shiozawa, Y. Terao, Estrogenic activity of alkylphenols, bisphenol S, and their chlorinated derivatives using a GFP expression system, Environ. Toxicol. Pharmacol. 19 (2005) 121–130.

[9] A.D. Dimou, V.A. Sakkas, T.A. Albanis, Trifluralin photolysis in natural waters and under the presence of isolated organic matter and nitrate ions: Kinetics and photoproduct analysis, J. Photochem. Photobiol. A 163 (2004) 473–480.

[10] G.P. Cao, J.L. Lu, G.Y. Wang, Photolysis kinetics and influencing factors of bisphenol S in aqueous solutions, J. Environ. Sci. 24 (2012) 846–851.

[11] G.P. Cao, R.L. He, Z.W. Cai, J. Liu, Photolysis of bisphenol S in aqueous solutions and the effects of different surfactants, React. Kinet. Mech. Catal. 109 (2013) 259–271.

[12] Y. Wang, J.H. Qu, Electrocatalytic reduction of nitrate in water with a palladium-modified copper electrode, Water Environ. Res. 78 (2006) 724–729.

[13] L. Jelínek, H. Parschová, Z. Matějka, M. Paidar, K. Bouzek, A combination of ion exchange and electrochemical reduction for nitrate removal from drinking water part I: Nitrate removal using a selective anion exchanger in the bicarbonate form with reuse of the regenerant solution, Water Environ. Res. 76 (2004) 2686–2690.

[14] K. Soropogui, M. Sigaud, O. Vittori, Alert electrodes for continuous monitoring of nitrate ions in natural water, Electroanalysis 18 (2006) 2354–2360.

[15] S. Israel, P. Engelbrecht, G. Tredoux, M. Fey, In situ batch denitrification of nitrate-rich groundwater using sawdust as a carbon source—Marydale, Water Air Soil Pollut. 204 (2009) 177–194.

[16] S. Goldstein, J. Rabani, Mechanism of nitrite formation by nitrate photolysis in aqueous solutions: The role of peroxynitrite, nitrogen dioxide, and hydroxyl radical, J. Am. Chem. Soc. 129 (2007) 10597–10601.

[17] G. Petriconi, H. Papee, Photoreactivity of aqueous anionic NO_x^- with hydrocarbons: Part II. Aromatic and aliphatic compounds in nitrite, Water Air Soil Pollut. 8 (1977) 217–224.

[18] J.M. Fisher, J.G. Reese, P.J. Pellechia, P.L. Moeller, J.L. Ferry, Role of Fe(III), phosphate, dissolved organic matter, and nitrate during the photodegradation of domoic acid in the marine environment, Environ. Sci. Technol. 40 (2006) 2200–2205.

[19] L.E. Jacobs, L.K. Weavers, Y.P. Chin, Direct and indirect photolysis of polycyclic aromatic hydrocarbons in nitrate-rich surface waters, Environ. Toxicol. Chem. 27 (2008) 1643–1648.

[20] J. Suzuki, T. Hagino, S. Suzuki, Formation of 1-nitropyrene by photolysis of pyrene in water containing nitrite ion, Chemosphere 16 (1987) 859–867.

[21] D. Vione, V. Maurino, E. Pelizzetti, C. Minero, Phenol photonitration and photonitrosation upon nitrite photolysis in basic solution, Int. J. Environ. Anal. Chem. 84 (2004) 493–504.

[22] G. Lente, Analytical solutions for the rate equations of irreversible two-step consecutive processes with second order later steps, J. Math. Chem. 53 (2015) 1759–1771.

[23] V. Matamoros, A. Duhec, J. Albaigés, J. Bayona, Photodegradation of carbamazepine, ibuprofen, ketoprofen and 17α-ethinylestradiol in fresh and seawater, Water Air Soil Pollut. 196 (2009) 161–168.

[24] Y. Chen, H. Li, Z.P. Wang, T. Tao, D.B. Wei, C. Hu, Photolysis of chlortetracycline in aqueous solution: Kinetics, toxicity and products, J. Environ. Sci. 24 (2012) 254–260.

[25] D.F. Wallace, L.H. Hand, R.G. Oliver, The role of indirect photolysis in limiting the persistence of crop protection products in surface waters, Environ. Toxicol. Chem. 29 (2010) 575–581.

[26] M.G. Steiner, C.F. Babbs, Quantitation of the hydroxyl radical by reaction with dimethyl sulfoxide, Arch. Biochem. Biophys. 278 (1990) 478–481.

[27] T. Charbouillot, M. Brigante, G. Mailhot, P.R. Maddigapu, C. Minero, D. Vione, Performance and selectivity of the terephthalic acid probe for ·OH as a function of temperature, pH and composition of atmospherically relevant aqueous media, J. Photochem. Photobiol. A 222 (2011) 70–76.

[28] C.G. Park, J.C. Kim, Effects of nitrate on the advanced UV photolysis of di(2-ethylhexyl) phthalate degradation in aqueous solution, Desalin. Water Treat. 47 (2012) 163–170.

[29] S. Kaneco, M.A. Rahman, T. Suzuki, H. Katsumata, K. Ohta, Optimization of solar photocatalytic degradation conditions of bisphenol A in water using titanium dioxide, J. Photochem. Photobiol. A 163 (2004) 419–424.

[30] J. Mack, J.R. Bolton, Photochemistry of nitrite and nitrate in aqueous solution: A review, J. Photochem. Photobiol. A 128 (1999) 1–13.

[31] C. Minero, V. Maurino, E. Pelizzetti, D. Vione, Assessing the steady-state [$\cdot NO_2$] in environmental samples: Implication for aromatic photonitration processes induced by nitrate and nitrite, Environ. Sci. Pollut. Res. Int. 14 (2007) 241–243.

[32] S. Rayne, K. Forest, K.J. Friesen, Mechanistic aspects regarding the direct aqueous environmental photochemistry of phenol and its simple halogenated derivatives, Environ. Int. 35 (2009) 425–437.

[33] G.F. Lv, D.C. Wu, R.W. Fu, Performance of carbon aerogels particle electrodes for the aqueous phase electro-catalytic oxidation of simulated phenol wastewaters, J. Hazard. Mater. 165 (2009) 961–966.